Scattering of ^{6}He from ^{197}Au, ^{nat}Ti, ^{27}Al, ^{nat}C, and ^{9}Be at $E = 8-9$ MeV

R. J. Smith, J. J. Kolata, K. Lamkin, and A. Morsad
Physics Department, University of Notre Dame, Notre Dame, Indiana 46556

K. Ashktorab, F. D. Becchetti, J. A. Brown, J. W. Janecke, W. Z. Liu, and D. A. Roberts
Physics Department, University of Michigan, Ann Arbor, Michigan 48109

(Received 3 October 1990)

Beams of ^{6}He ions having $E = 8.8-9.3$ MeV and intensity up to 2×10^{4} s^{-1} have been produced via the ^{9}Be(^{7}Li,^{6}He)^{10}B reaction. The beams had an energy resolution of 0.8 MeV full width at half maximum, 1-cm-diam spot size, and $\pm3°$ angular divergence. The first elastic-scattering data for ^{6}He from several targets are presented as examples of the use of this radioactive beam in secondary scattering experiments and their potential use for transfer or breakup reactions. Optical model parameters for ^{6}He are deduced by comparison with calculations using ^{6,7}Li and ^{4}He parameters. The data are well reproduced with ^{6}Li or ^{7}Li optical model parameters but not with those from ^{4}He.

I. INTRODUCTION

The quantitative development of nuclear astrophysics requires the measurement of nuclear reaction rates involving short-lived nuclei such as ^{8}Li and ^{6}He. As part of our program to produce beams of radioactive ions for these and other studies, and to utilize them for nuclear reactions,[1,2] we have measured the scattering of ^{6}He from a number of different target nuclei.

Scattering of ^{6}He is of considerable interest in nuclear physics. Because of the large binding energy of the alpha particle, the ^{6}He nucleus has been considered as an N-N-α nucleus with 3-body breakup from its first (unbound) excited state at 1.2 MeV.[3,4] In addition, it has been suggested that such a weakly bound neutron-rich nucleus may have a "neutron halo,"[5] enlarging its interaction radius in nuclear reactions. Initial measurements of ^{6}He reaction cross sections have not resolved this issue.[6] In addition to the theoretical interest in the three-body breakup of ^{6}He, there are a whole series of reactions of the type X(^{6}He,^{4}He) with very large positive Q values. We present here a survey of the yield, energy, and resolution for ^{6}He secondary-beam production and the first results of elastic scattering of 8.7–9.3-MeV ^{6}He beams (incident energy) from ^{197}Au, ^{48}Ti, ^{27}Al, ^{12}C, and ^{9}Be. The production reaction was ^{9}Be(^{7}Li,^{6}He)^{10}B, which has a Q value of -3.38 MeV, and the ^{6}He ions were produced as a parasite beam to ^{8}Li production.

II. EXPERIMENTS

The experimental apparatus used to collect and focus radioactive beams has been described in detail elsewhere.[1] Recent additions to this apparatus are an adjustable z (beam axis) beam stop in the midplane chamber and a rotating primary target assembly.[7] The z-movable stop consists of a 3-cm-diameter disk which can be positioned under vacuum at distances between 156 and 190 cm from the primary target. This may be used to filter out lower rigidity ions including primary-beam scattered particles. Although increasing the magnetic field of the solenoid may achieve the same ends, the improved beam purity often comes at the expense of the secondary-beam focus. The yield and energy resolution of the secondary ^{6}He beam was investigated as a function of solenoid current and z-stop position for the ^{9}Be(^{7}Li,^{6}He) reaction at three ^{7}Li bombarding energies. In addition, these beams were used to measure elastic-scattering cross sections from a number of targets and so comprise the most comprehensive set of scattering data for ^{6}He so far available.

III. EXPERIMENTAL RESULTS

Beams of ^{7}Li of energy 14.63, 16.1, and 17 MeV were used to produce ^{6}He secondary beams. The first excited state of ^{6}He is unstable to three-body breakup. Only with a ^{7}Li beam energy of 14.63 MeV are the ^{6}He and ^{10}B, populated in their ground states, brought to a focus at the secondary target. At the other ^{7}Li energies the ^{10}B residual nucleus must carry away 2.5–3.5 MeV of excitation energy. This is necessary for the ^{6}He to be bent by the solenoid magnetic field to a secondary-target focus. It should be noted that most of the results reported here were obtained with parasite beams to experiments with ^{8}Li reported elsewhere[7–9] and were therefore not particularly optimized for ^{6}He production.

The production targets used with the 14.63 and 17.0-MeV ^{7}Li beams were 12.7-μm-thick ^{9}Be foils. The yield and energy resolutions are presented in Table I. In all cases the solenoid angular acceptance was 5°–11° corresponding to a solid angle of 94 msr. Also included are the parameters for the 8.2-MeV ^{6}He ion beam reported elsewhere.[10] Figure 1 shows the ΔE-E_R signature and beam profile of ^{6}He.

There are essentially two methods employed to measure the yield of a secondary beam (expressed as ^{6}He ions s^{-1} $e\mu$A^{-1} ^{7}Li). The first method measures the yield directly: a large-area ΔE-E_R detector is placed at 0°, and the number of secondary ions accepted and transmitted

TABLE I. Experimental parameters for 17-MeV ^{7}Li on ^{9}Be(^{7}Li,^{6}He)^{10}B using a 12.7-μm ^{9}Be primary target and 5°–11° solenoid angular acceptance.

Run No.	Incident ^{6}He energy	Resolution (MeV)	Solenoid current (A)	Yield (^{6}He s^{-1} e mA^{-1})[a]	Solid-state detector (Ω)
1	8.84	0.74	113.0	5350±900	13.5
2	9.39	1.19	115.5	11 210±1610	6.7
3	9.00	0.71	113.0	5760±1330	6.7

[a]These data represent a conversion efficiency (^{6}He/^{7}Li) of $(2.6-9.2)\times 10^{-9}$.

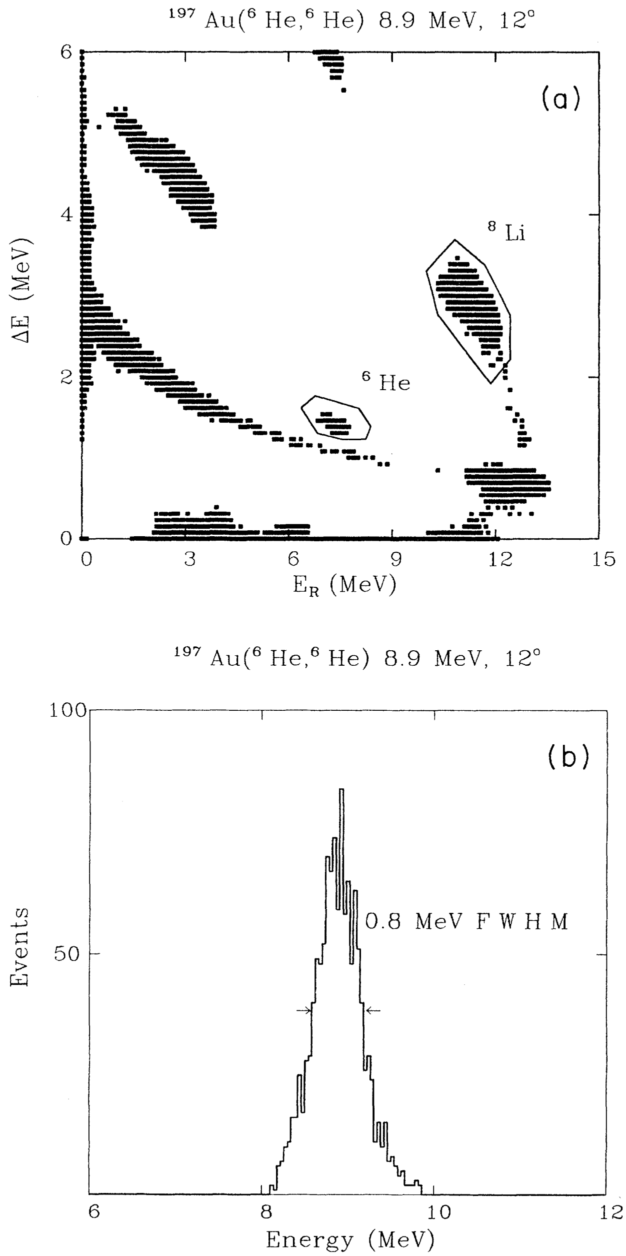

FIG. 1. (a) ΔE vs E_r for the scattering of a 8.9-MeV ^{6}He secondary beam on ^{197}Au at 12°. (b) Energy profile for scattered ^{6}He.

through the solenoid is measured. Since the detector is some 12 cm farther back than the secondary-target focal point, the field has to be reduced by around 1.1% to simulate a secondary-target focus. The count rate tolerance of the solid-state detectors greatly restricts this method and makes the method time consuming. The second method (more commonly used) measures the Rutherford scattering of the secondary beam from a gold target at several detector angles. This has the added advantage of providing an on-line secondary-beam flux calibration. However, with ^{6}He there is a danger that flux may be lost to Coulomb breakup of the ^{6}He ions from their first excited state, giving a false value for both the ^{6}He yield and the secondary-beam intensity and, therefore, of the measured cross sections. We have performed a survey of direct versus indirect yields for ^{6}He production using a 16.1-MeV ^{7}Li beam and 6-μm ^{9}Be target (to simulate ^{6}He production from a 17-MeV ^{7}Li beam on 12.7 μm ^{9}Be). The results of this survey are 1444±391 ^{6}He $s^{-1} e\mu A^{-1}$ for the indirect yield and 1503±198 ^{6}He $s^{-1} e\,\mu A^{-1}$ for the direct yield. It can be seen that the two values agree, and that therefore there is no indication of significant Coulomb breakup of the ^{6}He beam at this energy.

The ^{6}He yields at 8.2–9.3 MeV ranged from 19 000 to 5800 ^{6}He ions $s^{-1} e\,\mu A^{-1}$ of ^{7}Li from 12.7 μm ^{9}Be. The largest yields result from production with both ^{6}He and ^{10}B left in their ground states. The maximum ^{6}He beam intensity achieved was 2×10^{4} s^{-1}.

Finally, the first systematic measurements of elastic scattering of ^{6}He beams from ^{197}Au, ^{nat}Ti^{2}H$_2$, ^{27}Al, ^{9}Be, and ^{nat}C are presented. These are the results of the three sets of experiments defined in Table I. The differential cross sections for the ^{12}C and ^{9}Be targets, at different nominal scattering angles, are presented in Table II. Since the position-sensitive detectors spanned 5.3° and 7.6°, respectively, they were divided into 1–2° slices to provide more information on the angular distributions.

Unlike the case for conventional nuclear elastic-scattering experiments, our beam spans the angular range from $\frac{5}{3}$° to $\frac{11}{3}$° in the laboratory system. (A factor of $\frac{1}{3}$ comes from the angular magnification of the solenoid.) This means that, given the rapid fall in scattering cross section with increasing angle, the effective beam angle is weighted toward a small angle. The nominal detection angles are therefore typically 0.5°–2.0° larger than the cross-section-weighted scattering angles.

The problem then becomes how to correct for this to

TABLE II. Nominal detection angles (θ_{lab}) and laboratory differential cross sections (mb sr^{-1}) for ^{6}He scattering from ^{9}Be and ^{nat}C. ^{6}He energies are given for the centers of the target foils. Note that these values have not been corrected for beam divergence or detector width. The true (forward-angle-weighted) angles will be smaller than those quoted here.

	9.18-MeV ^{6}He on ^{12}C (No. 2)			8.79-MeV ^{6}He on ^{12}C (No. 3)	
θ (lab)	$\frac{d\sigma}{d\Omega}$ (b/sr)	Error	θ (lab)	$\frac{d\sigma}{D\Omega}$ (b/sr)	Error
12.9	22.9	2.64	9.9	81.7	11.4
13.9	17.4	1.81	10.9	45.3	6.68
15.0	9.30	1.27	12.0	18.1	4.04
16.1	5.07	0.98	12.4	13.7	2.11
17.1	4.57	1.18	13.1	11.8	3.41
17.4	3.25	0.38	14.1	11.2	4.24
20.0	1.29	0.29	15.0	6.27	1.74
22.4	0.71	0.15	17.4	2.88	0.53
22.6	1.04	0.21	17.6	3.58	1.08
25.0	0.50	0.15	20.0	2.06	0.55
27.6	0.28	0.09	22.6	0.89	0.30
30.0	0.17	0.06			
	8.20-MeV ^{6}He on ^{9}Be (No. 2)			8.24-MeV ^{6}He on ^{9}Be (No. 3)	
17.3	2.05	0.36	10.9	46.6	6.07
20.0	1.05	0.17	12.0	19.6	3.77
22.7	0.51	0.18	12.9	8.32	1.03
23.3	0.38	0.10	13.1	14.2	3.35
26.0	0.39	0.07	13.9	5.04	0.63
28.7	0.19	0.07	14.1	3.85	2.22
29.3	0.29	0.09	15.0	2.68	0.44
32.0	0.21	0.05	16.1	1.97	0.39
34.7	0.08	0.05	17.1	1.02	0.36
			20.0	0.65	0.09
			25.0	0.25	0.08

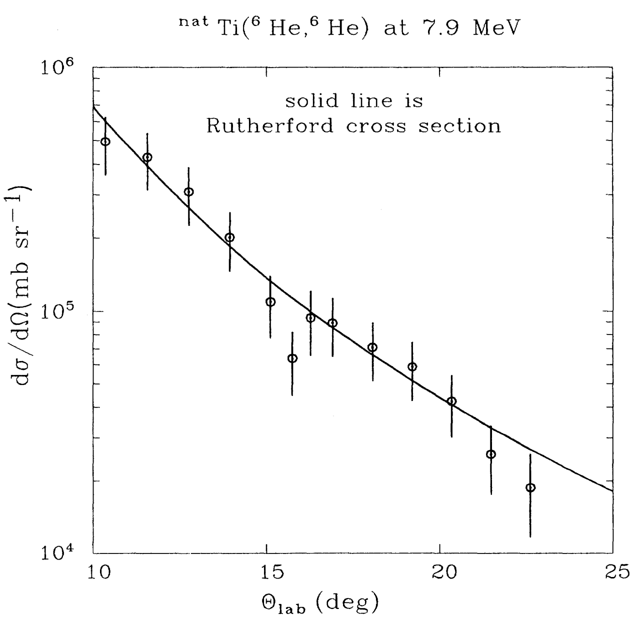

FIG. 2. Fit to experimental angular distribution for scattering of 7.9-MeV ^{6}He from $^{nat}TiH_2$. The distribution follows Rutherford scattering within the overall experimental errors. Note that the experimental points have been multiplied by 1.10 for the fit.

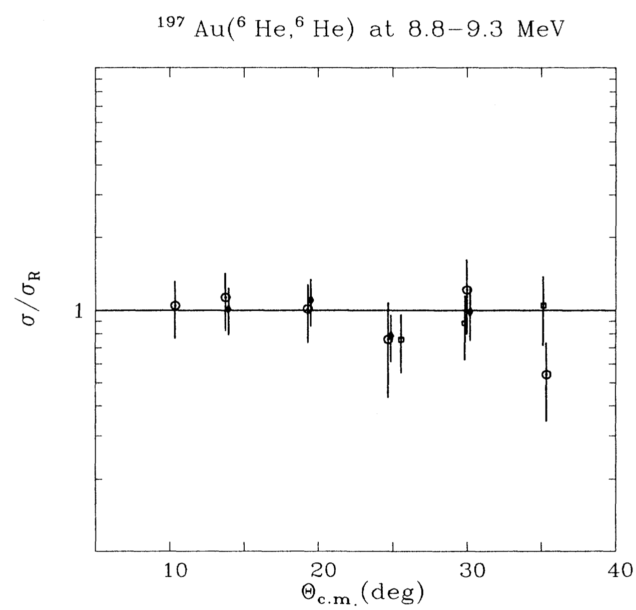

FIG. 3. Rutherford scattering of ^{6}He:^{197}Au(^{6}He,^{6}He) at ^{6}He energies of 8.75, 8.9, and 9.3 MeV.

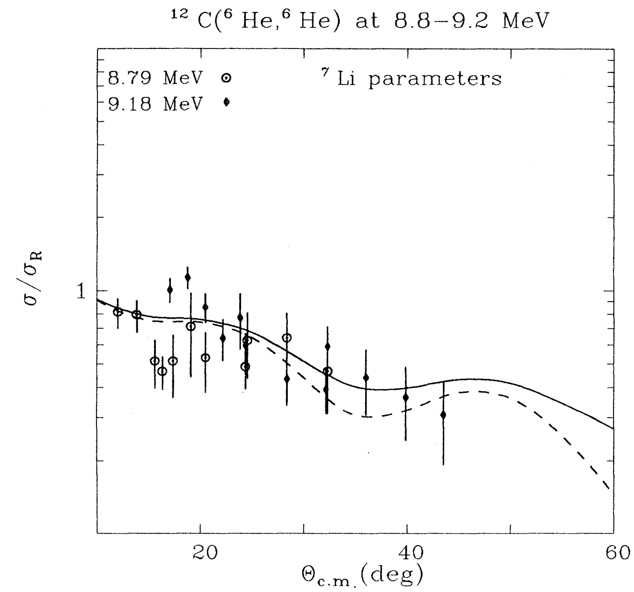

FIG. 4. Elastic scattering of ^{6}He:^{12}C(^{6}He,^{6}He) at ^{6}He energies of 8.8 and 9.2 MeV with OM angular distributions using the ^{7}Li parameters given in Table III. The solid curve is for the global potential; the dashed curve is for the local potential. Both are for 8.99-MeV ^{6}He ions.

obtain a true detection angle. To do this, two assumptions have been made: (1) that the angular distribution from 5° to 11° is flat and (2) that the angular distribution is, overall, a smooth function of $1/\sin^{n}(\theta_{c.m.})$. While, clearly, neither is true, they are fair first approximations.

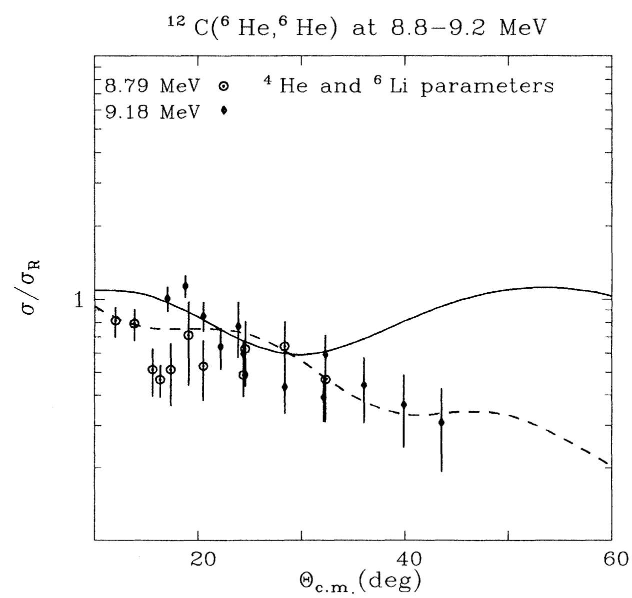

FIG. 5. Elastic scattering of ^{6}He:^{12}C(^{6}He,^{6}He) at ^{6}He energies of 8.8 and 9.2 MeV with OM angular distributions using the ^{4}He and ^{6}Li parameters given in Table III. The solid curve is for the ^{4}He potential; the dashed curve is for the ^{6}Li potential. Both are for 8.99-MeV ^{6}He ions.

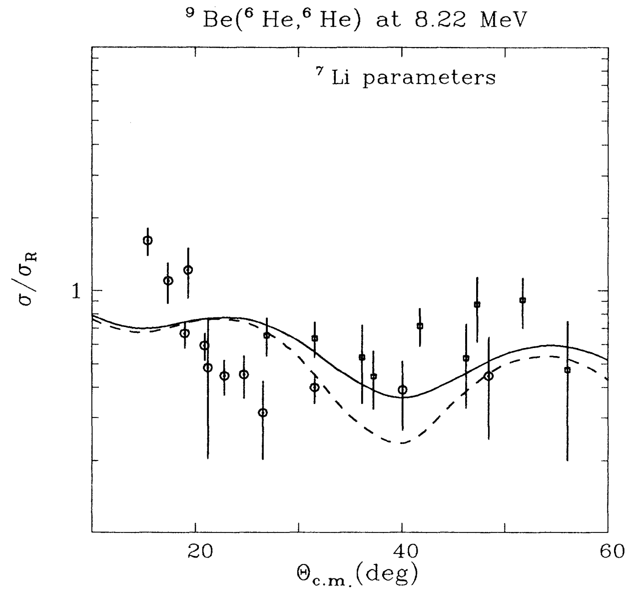

FIG. 6. Elastic scattering of ^{6}He:^{9}Be(^{6}He,^{6}He) at a ^{6}He energy of 8.22 MeV with OM angular distributions using the ^{7}Li parameters given in Table III. The solid curve is for the global potential; the dashed curve is for the local potential.

For example, a fit to the angular distribution of 7.9-MeV ^{6}He on ^{nat}Ti is presented in Fig. 2. The next step is to divide the divergent beam annulus into thin slices and calculate the weighted mean θ_{det}-θ_{beam}. The computed values of the exponent n were 4 (as expected) for ^{197}Au,

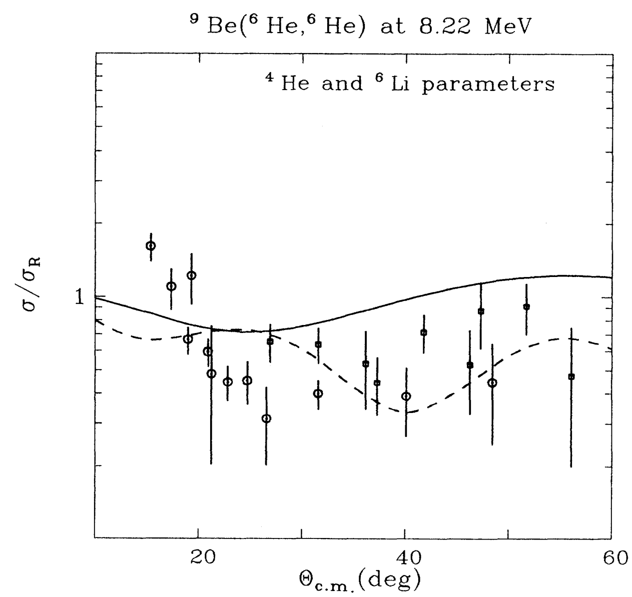

FIG. 7. Elastic scattering of ^{6}He:^{9}Be(^{6}He,^{6}He) at a ^{6}He energy of 8.22 MeV with OM angular distributions using the ^{4}He and ^{6}Li parameters given in Table III. The solid curve is for the ^{4}He potential; the dashed curve is for the ^{6}Li potential.

TABLE III. OM potentials for ^{6}He elastic scattering.

Potential	r_{0r} (fm)	a_r (fm)	r_{0i} (fm)	a_i (fm)	V_r (fm)	W_i (fm)	r_{0C} (fm)
^{7}Li global	0.60	0.80	1.31	0.72	167.0	9.57	1.25
^{7}Li	0.64	0.82	1.16	0.77	188.0	13.0	0.69
^{4}He (C)	0.53	0.50	0.53	0.50	150.0	1.50	0.36
^{4}He (Be)	0.47	0.50	0.47	0.50	128.4	3.35	0.46
^{6}Li	0.61	0.79	1.34	0.62	154.0	4.40	1.25

^{nat}Ti, and ^{27}Al, and 5 for ^{nat}C and ^{9}Be.

The elastic-scattering results are presented versus c.m. scattering angle in Figs. 3 (^{197}Au), 4,5 (^{nat}C), and 6,7 (^{9}Be). Illustrated on the plots are the errors propagated from statistical uncertainties. The errors from the absolute normalizations are not included since these will not alter the shape of the angular distributions. The absolute normalization errors vary from 15% to 19%. Elastic-scattering cross sections for ^{6}He from Au, Ti, and Al follow Rutherford values closely. Scattering from C and Be shows clear deviations from Rutherford scattering. To investigate this behavior we performed some standard optical model (OM) calculations with the programs CUPID (Ref. 11) and PTOLEMY (Ref. 12) with parameters, taken from ^{7}Li, ^{6}Li, and ^{4}He scattering,[13–15] which are shown in Table III. The optical model potential is of the form $U(r)=V_{\rm Coul}-(V_r+iW_i)f(r)$, where W_i is a volume absorption potential. The optical model uses a Woods-Saxon form factor:

$$f(r)=\left[1+\exp\frac{r-R}{a}\right]^{-1},$$

where R is the sum of the nuclear radii and a is the diffuseness parameter. In all cases the radius parameters r_{0r} (real), r_{0i} (imag) and r_{0C} (Coul) are defined by the equation

$$R=r_0(A_p^{1/3}+A_t^{1/3}) .$$

From these calculations it appears that the angular distributions for ^{6}He scattering are very similar to those predicted using ^{7}Li or ^{6}Li OM parameters. Angular distributions using ^{4}He OM potentials reproduce the data much less well.

IV. CONCLUSIONS

Beams of ^{6}He were produced from the ^{9}Be(^{7}Li,^{6}He) reaction between 5° and 11° outgoing angle, with a rate of 6000–19 000 ions $s^{-1}\,e\,\mu A^{-1}$ and with an energy resolution of 0.8 MeV. These beams have allowed us to perform the first systematic study of ^{6}He elastic scattering from a variety of targets. The angular distributions for ^{6}He elastic scattering are well reproduced using ^{7}Li or ^{6}Li optical model parameters. Angular distributions using ^{4}He optical model parameters do not reproduce the data well.

It is hoped, with the aid of an energy-loss absorber to improve our ^{6}He yield, and that future experiments will pursue a new generation of ^{6}He-induced reactions such as (^{6}He,^{4}He), for example.

[1] J. J. Kolata, A. Morsad, X. J. Kong, R. E. Warner, F. D. Becchetti, W. Z. Liu, D. A. Roberts, and J. W. Janecke, Nucl. Instrum. Methods B **40/41**, 503 (1989).

[2] F. D. Becchetti, W. Z. Liu, D. A. Roberts, J. W. Janecke, J. J. Kolata, A. Morsad, X. J. Kong, and R. E. Warner, Phys. Rev. C **40**, 1104 (1989).

[3] W. C. Parke and D. R. Lehman, Phys. Rev. C **29**, 2319 (1984).

[4] J. J. Bevelacqua, Phys. Rev. C **33**, 699 (1986).

[5] P. G. Hanson and B. Jonson, Europhys. Lett. **4**, 409 (1987).

[6] M. C. Saint-Laurent *et al.*, Z. Phys. A **332**, 457 (1989).

[7] J. Brown, F. D. Becchetti, W. Z. Liu, J. W. Janecke, D. A. Roberts, J.J. Kolata, R. J. Smith, K. Lamkin, and A. Morsad, in *Proceedings of The First International Conference on Radioactive Nuclear Beams, 1989,* edited by W. D. Myers, J. M. Nitschke, and E. D. Norman (World Scientific, Singapore, 1990), p. 201.

[8] F. D. Becchetti, J. Brown, W. Z. Liu, D. A. Roberts, J. J. Kolat, R. J. Smith, K. Lamkin, A. Morsad, and R. E. Warner, in Ref. 7, p. 305.

[9] W. Z. Liu, F. D. Becchetti, J. Brown, D. A. Roberts, J. J. Kolata, A. Morsad, R. J. Smith, and X. J. Kong, in Ref. 7, p. 499.

[10] W. Liu, Ph.D thesis, University of Michigan, 1990 (unpublished).

[11] J. R. Comfort, Comput. Phys. Commun. **16**, 35 (1978).

[12] M. H. MacFarlane and S. C. Pieper, PTOLEMY: A program for Heavy Ion Direct-Reaction Calculations, Report No. ANL-76-11. Rev. 1, 1978.

[13] M. F. Vineyard, J. Cook, K. W. Kemper, and M. N. Stephens, Phys. Rev. C **30**, 916 (1984).

[14] P. Schumacher, N. Ueta, H. H. Duhm, K. I. Kubo, and W. J. Klages, Nucl. Phys. **A212**, 573 (1973).

[15] C. M. Perey and F. G. Perey, At. Data Nucl. Data Tables **17**, 80 (1976).